Converse flexoelectric effect in a bent-core nematic liquid crystal

J. Harden,[1] R. Teeling,[2] J. T. Gleeson,[2] S. Sprunt,[2] and A. Jákli[1]
[1]*Chemical Physics Interdisciplinary Program and Liquid Crystal Institute, Kent State University, Kent, Ohio 44242, USA*
[2]*Department of Physics, Kent State University, Kent, Ohio, 44242, USA*
(Received 22 May 2008; published 2 September 2008)

Flexoelectricity is a unique property of liquid crystals; it is a linear coupling between electric polarizations and bend and/or splay distortions of the direction of average molecular orientation. Recently it was shown [J. Harden *et al.*, Phys. Rev. Lett. **97**, 157802 (2006)] that the bend flexoelectric coefficient in bent-core nematic liquid crystals can be three orders of magnitude higher than the effect with calamitic (rod-shaped) molecular shape. Here we report the converse of the flexoelectric effect: An electric field applied across a bent-core liquid crystal sandwiched between thin flexible substrates produces a director distortion which is manifested as a polarity-dependent flexing of the substrates. The flex magnitude is shown to be consistent with predictions based upon both the measured value of the bend flexoelectric constant and the elastic properties of the substrates. Converse flexoelectricity makes possible a new class of microactuators with no internal moving parts, which offers applications as diverse as optical beam steering to artificial muscles.

DOI: 10.1103/PhysRevE.78.031702 PACS number(s): 61.30.Cz, 61.30.Gd, 84.37.+q

I. INTRODUCTION

The discovery of the mesogenic properties of bent-core molecules has opened up a major new and exciting dimension in the science of thermotropic liquid crystals (LCs). Seminal findings—having broad implications for the general field of soft condensed matter—include the observation of ferroelectricity and spontaneous breaking of chiral symmetry in smectic phases composed of molecules that are not intrinsically chiral [1]. To date, most of the research effort has focused on bent-core smectics; liquid phases exhibiting purely orientational order (nematic phases) are rather uncommon in bent-core compounds. However, recently a number of new bent-core compounds with nematic phases (BCNs) have been synthesized [2–4]. Simultaneously there has been a surge in theoretical studies [5–8] predicting intriguing new thermotropic nematic and isotropic structures. These include biaxial phases, orientationally ordered, but optically isotropic phases, and even spontaneously chiral and polar liquid phases; all are made theoretically possible by the bent shape of the molecules. On the experimental front, several recent studies [9,10] have shown that, although their dielectric and Frank elastic constants ($\Delta\varepsilon \sim -1.6, K_{11} \sim K_{33} \sim 2.3 \times 10^{-12}$ N) and the diamagnetic anisotropy [$\chi_a = 1.7 \times 10^{-7}$ (SI)] are comparable to standard calamitic liquid crystals, many properties of BCNs are quite unusual. For example, in one particularly well-studied compound [4-chloro-1,3-phenylene bis[4-(10-decenyloxy)benzoyloxy] benzoate, shown in Fig. 1(a) and denoted ClPbis10BB], it has been observed that, in comparison to typical calamitics, the leading coefficient in a Landau—de Gennes free energy is 30 times lower [10]; the viscosity associated with nematic order fluctuations is 10 times higher [10], the flow viscosity is 100 times higher [11], and the conductivity anisotropy is 100 times lower. Perhaps most intriguing, however, is the recent report [12] in BCNs of giant flexoelectricity [13]. The flexoelectric effect [13] is characterized by two coefficients e_1 and e_3, coupling splay and bend director distortions, respectively, to an induced polarization through the following relation: $\boldsymbol{P} = e_1 \boldsymbol{n}(\nabla \cdot \boldsymbol{n}) + e_3(\nabla \times \boldsymbol{n}) \times \boldsymbol{n}$, where $\boldsymbol{n}$ is the director, a unit vector field denoting the direction of average molecular orientation. Since the coefficient e_3 was found to be three orders of magnitude larger in ClPbis10BB than in standard calamitic (rodlike) nematic compounds, BCNs offer remarkable new technological prospects for conversion of mechanical to electrical energy.

Because flexoelectricity is a linear relation between polarization and gradients of $\boldsymbol{n}$, symmetry predicts that the inverse of the effect—i.e., orientational distortion or flexing of a film produced by application of an electric field—should also occur. Such a "converse flexoelectric effect" so far has been detected only in solids such as barium strontium titanates subjected to inhomogeneous electric fields [14] and in black bilayer lipid membranes, in which a 20 m^{-1} spherical curvature [15–17] of the film was reportedly induced under an applied field of 55 V/μm. The latter measurement corresponds to a splay flexoelectric coefficient [18] of $e_1 \sim 100$ pC/m, which is an order of magnitude larger than

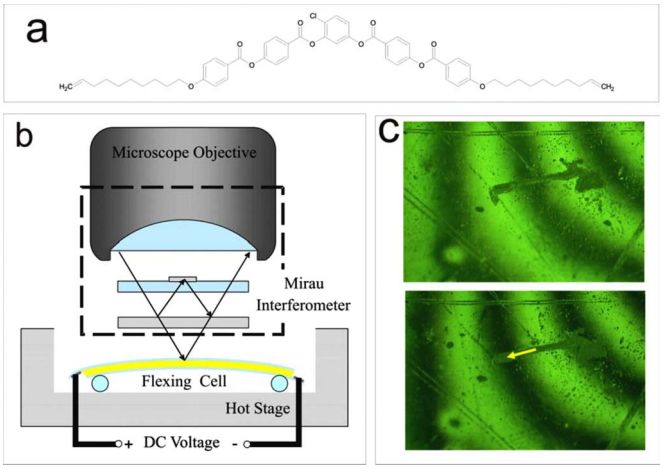

FIG. 1. (Color online): The molecular structure of the studied material (a); the experimental setup (b); and the typically observed fringe shifts corresponding to an upward deflection (c).

typical for calamitic thermotropic liquid crystals, but still two orders of magnitude smaller than the bend flexoelectric coefficient $e_3 \sim 60$ nC/m observed in the BCN ClPbis10BB [12]. The converse flexoelectricity of BCNs therefore not only offers a potentially larger effect than that in the lipid membranes, but is also different in that it would produce a cylindrical curvature of the film and would therefore not be as susceptible to rupture as the lipid membranes. Moreover the single component BCNs are easily contained and aligned between flexible, compliant substrates, making them far more practical for applications such as electromechanical actuators and beam steering devices. In this paper we present the measurement of converse flexoelectricity of a thermotropic bent-core nematic liquid crystal (ClPbis10BB), and demonstrate a substantial effect (0.001 m^{-1} curvature induced by a 4 V/μm applied field) that is fully consistent with the previously measured flexoelectric coefficient.

II. EXPERIMENTAL TECHNIQUE

For our measurements the bent-core compound ClPbis10BB [Fig. 1(a)] was synthesized at Organic Synthesis Facility in Kent State's Liquid Crystal Institute using the procedure described in Refs. [19,20]. ClPbis10BB is monotropic, exhibiting a nematic phase upon cooling between 72 °C and about 57 °C (depending on cooling conditions). The two arms of the molecule are relatively flexible, because the outer benzene rings are separated by ester groups.

Sample cells were constructed from two 100 μm thick flexible Mylar substrates with ITO sputtered on the surfaces as conducting layers. Polyvinyl alcohol was spin coated and rubbed as an alignment layer on top of the ITO. The substrates were 14 mm × 21 mm, while the electrode region was 12 mm × 18 mm. The cell gap was set to 25 μm by glass fiber spacers sparsely distributed throughout the electrode region. The liquid crystal ClPbis10BB was capillary filled into the cells. The filled cells were then placed on two 2 mm diameter glass rods which were mounted in an Instec Hot stage HS 2000 regulated by an Instec Heat Controller. The electrical leads of the sample were connected to a BK precision dc power supply and a voltage amplifier. Voltages applied across the cell were measured with an HP 34401A multimeter.

A Leitz Mirau interferometer mounted to the objective port of an Olympus BX51 microscope (used in reflection mode) was employed to measure the upward or downward deflections of the sample induced by the applied voltage. Figure 1 gives a schematic of the experimental apparatus. The interferometer was adjusted such that from 3 to 5 fringes were viewable on the video display. Images were recorded at 0 V, and at video rates for about 2 seconds after voltages were applied.

When voltage was applied to the sample, the interference fringes were observed to shift either to the left (corresponding to an upward displacement of the center of the cell) or to the right (a downward displacement). The direction of the motion could be verified by using the fine adjustment of the microscope focus: Moving the sample stage slightly up (down) yielded fringes that shifted left (right) (Fig. 1). A green filter (532 nm) was used to improve the fringe resolution. The theoretical limit of the accuracy of the interferometer is 3 nm [21]; however, vibrations and thermal fluctuations in the set up extended this to about 5 nm even when the microscope was mounted on a vibration damped optical table. This error is still much smaller than the experimentally observed sample deflections, which were typically in the 10 nm to 200 nm range for the relevant applied voltages.

The amplitude of the sample's maximum deflection, d, was determined from the measured relative fringe displacement m, defined as the ratio of the fringe shift to the distance between fringes, i.e., $d = m\lambda/2n$, where $\lambda = 532$ nm is the wavelength. We measured deflections under both positive and negative potential differences V between the upper and lower electrodes as a function of temperature and the amplitude of the applied voltage.

III. RESULTS AND DISCUSSION

At high temperatures, deep in the isotropic phase, only downward deflections of the top substrate are seen under applied voltages of both signs. We assume that in the isotropic phase far from the nematic transition, there can be no converse flexoelectric effect, and the downward deflection is due to the Coulomb attraction between the conducting substrates; this attraction results from both the induced charge on the conducting coatings at nonzero V, and static charge in the mylar. The presence of static charge is indicated by a different value of downward deflection for different polarity of V in the isotropic phase far from the nematic. The downward deflection due only to the induced charge is isolated by averaging the deflection at reversed polarities; the deflection due to the static charge is then one-half the difference between the deflections at reversed polarities. The deflection due to static was measured at a temperature well above the clearing and subtracted from all subsequent measurements as a temperature-independent baseline correction.

After correcting for static charge, our raw data corresponds to measurements of the voltage-dependent deflection under both polarities, $d(+|V|)$ and $d(-|V|)$. The asymmetric and symmetric parts of the deflections d_a and d_s are defined as

$$d_a = \frac{d(+|V|) - d(-|V|)}{2}, \quad d_s = \frac{d(+|V|) + d(-|V|)}{2}. \quad (1)$$

The polarity-dependent d_a describes a flexing of the plate due to converse flexoelectricity. Following the original definition of the flexoelectricity by Meyer [13], the flexoelectric coefficients is positive if $d_a > 0$ and negative if $d_a < 0$. When the symmetric part of the deflection is negative ($d_s < 0$), it describes squeezing of the material out from the electrode area.

The temperature dependence of the displacements d_a and d_s are shown in Fig. 2.

We see that in the temperature range well into the isotropic phase, the flexing with 90 V applied is immeasurably small, but, at about 5 °C above the clearing point it starts increasing, until a maximum of about 125 nm is reached at 5 °C–7 °C below the isotropic-nematic transition. Be-

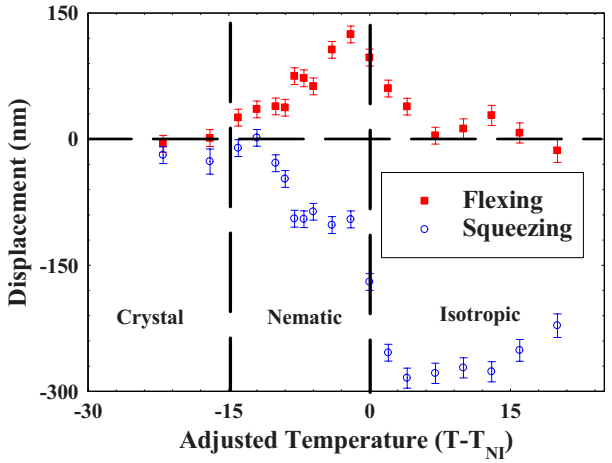

FIG. 2. (Color online) Displacements d_a (solid squares) and d_s (hollow circles) of the sample at 11 mm from edge and ± 90 V applied.

yond this, it decreases to zero at the crystallization temperature, because the electric field cannot rotate the director. The magnitude of the squeezing is larger in the isotropic than in the nematic phase, and it is zero in the crystal phase. The disappearance of the squeezing upon crystallization can be attributed to the suppression of the flow of the material.

We examined the voltage dependence of $|d_a|$ and $|d_s|$ at the middle cell position and the temperature (approximately 8 °C below T_{NI}) where the flexing was measured to be large and the squeezing is relatively small. The results are shown in Fig. 3.

As shown in Fig. 3, the voltage dependence of $|d_a|$ due to flexing is acceptably linear above a threshold of about 10 V. On the other hand, $|d_s|$ due to squeezing shows no threshold with a roughly quadratic increase at lower voltages, and returns to almost zero above 60 V. Optical observations reveal a gradual formation of a stripe pattern at about 30 V due to the onset of an electrohydrodynamic instability previously described by Wiant *et al.* [9]. At increasing voltages the

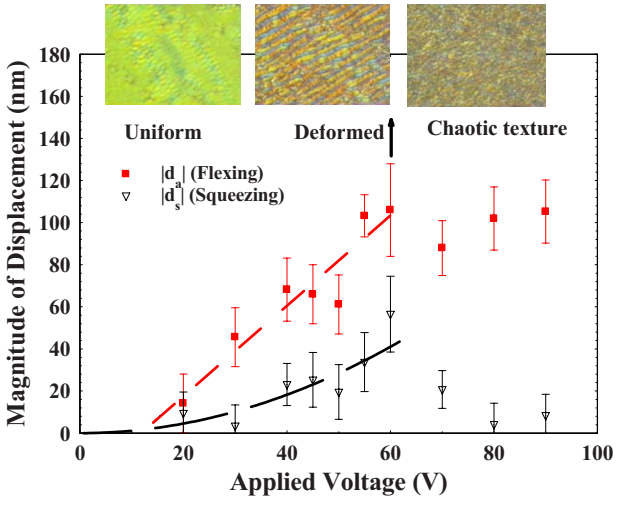

FIG. 3. (Color online): Voltage dependence of flexing and squeezing 8 °C below T_{NI} and 1 mm from the center of the cell, and the corresponding textures seen in polarizing microscope.

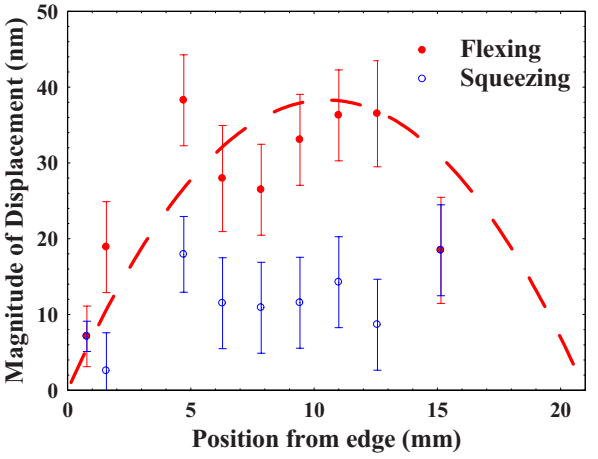

FIG. 4. (Color online) The spatial dependence of the displacements due to flexing and squeezing as measured at the distance from one of the edges along a line in the middle of the electrode area. The liquid crystal is 4 °C below T_{NI} and the applied dc voltage was 40 V. Dashed line is a fit assuming the small displacement $d(x)$ is on the arc of a semicircle with radius R much larger than of the length of the film L, i.e., $d=(Lx-x^2)/2R$.

stripe spacing narrows and the texture becomes chaotic at around 60 V, where the squeezing effect starts to decrease. Although we do not understand this decrease, we speculate that it may be caused by the suppression of flow as the chaotic pattern emerges. Due to the strong planar anchoring of the liquid crystal (LC) the alignment is not disturbed at the surface, explaining why the polarization charges at the substrates due to flexoelectricity are not influenced so much by the electrohydrodynamic instability.

Figure 4 shows the spatial profiles of $|d_a|$ and $|d_s|$ as a function of the distance measured along a line across the cell parallel to the rubbing direction and perpendicular to the supporting rods. (Zero position corresponds to the position of one of the supporting rods.) The data were taken at a temperature 4 °C below T_{NI} and for $V=40$ V. They reveal maximum flexing deflection in the middle of the cell as one would expect for a support geometry in which the cell edges are supported at a fixed (zero) vertical displacement.

Profile experiments were also done along the orthogonal direction—i.e., when the supporting rods of the cell were placed parallel to the rubbing direction. In this case there was no observed bending showing that in this geometry the supporting rods do not allow bending. This establishes that the flexing axis is perpendicular to the director, i.e., the flexing is associated with a bend deformation of the director, corresponding to the involvement of the bend flexoelectric constant e_3. From the profile in Fig. 4 we can estimate the minimum of the cell curvature radius R utilizing that for small displacements $R=(Lx-x^2)/2d$, where d is the displacement, L is the length of the substrate, and x is the distance from the edge of the substrate. From the fit to flexing profile in Fig. 4 we obtain $R \sim 1300$ m.

Using the above measurements we can calculate the bend flexoelectric coefficient, e_3. We equate the converse flexoelectric energy E_{flex} with the bending energy E_{bend} of the mylar substrates. The energy of a cylindrically bending plate

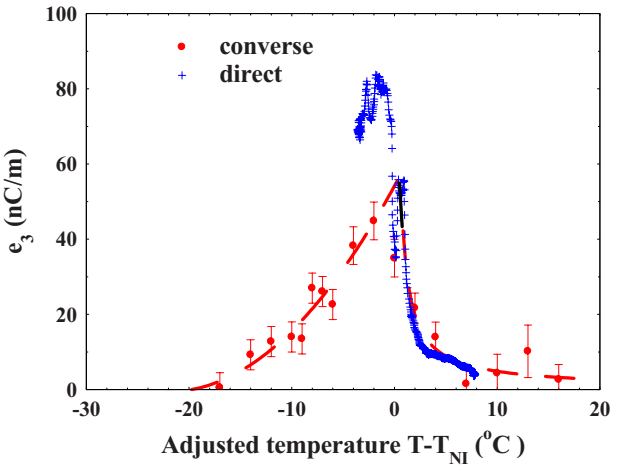

FIG. 5. (Color online) Comparison of the temperature dependences of the bend flexoelectric coefficient measured by the direct and converse flexoelectric effects.

having thickness h and Young modulus Y can be written as [22]

$$E_{\text{bend}} = \frac{A_{\text{sub}} Y}{2R^2(1-\sigma^2)} \int_{-h/2}^{h/2} z^2 dz = \frac{Yh^3}{12} \frac{A_{\text{sub}}}{2R^2(1-\sigma^2)}, \quad (2)$$

where R is the radius of curvature, $A_{\text{sub}}=296$ mm^2 is the area of the substrates, $\sigma \sim 0.4$ [23] is Poisson's ratio of mylar, $Y=3.3$ GPa [24,25] and $h=100$ μm. On the other hand, the flexoelectric energy for bend distortion of the director is

$$E_{\text{flex}} = \frac{e_3}{R} V A_{\text{LC}}, \quad (3)$$

where e_3 is the bend flexoelectric constant, V is the applied electric potential, and $A_{\text{LC}}=216$ mm^2 is the area of the liquid crystal in the electrode area. Equating (2) and (3) we can express e_3 as

$$e_3 \approx \frac{A_{\text{sub}}}{A_{\text{LC}}} \frac{dYh^3}{12(Lx-x^2)(1-\sigma^2)V}. \quad (4)$$

Then, from the temperature dependence of the flexing displacement (Fig. 2) we obtain the temperature dependence of e_3 as shown in Fig. 5. This is plotted together with the temperature dependence of e_3 obtained from our previous, direct flexoelectric measurements [12,26] in ClPbis10BB. Here it is important to note that whereas from the direct measurements only the magnitude of the flexoelectric constant could be determined, from the converse measurement we could determine that the sign of e_3 is positive by noting the sign of field and the direction of bending [as shown in Fig. 1(b)] and by comparing this with the definition of the sign of flexoelectricity [13]. This is consistent with the molecular structure that has a dipole pointing along the bow axis. From Fig. 5 it can be seen that the flexoelectric coefficients measured from the direct and converse effects have the same order of magnitude, although the coefficient measured from the converse effect is somewhat smaller. The difference could easily be due to different alignment conditions related to the electrohydrodynamic instability. Another important difference is that during measurements of the converse effect the material crystallized at lower temperatures, because of much less mechanical disturbances than during the direct measurements. We note that the slope of 1.4 nV/C obtained from the voltage dependence shown in Fig. 3 also gives $e_3 \approx 40$ nC/m at 4 °C below T_{NI}, in complete agreement with Fig. 5. It is important to note that the bending modulus is cubic with thickness. Using thinner substrates will drastically reduce the mechanical resistance to the converse flexoelectric effect and would substantially increase the amplitude of the bending.

Finally we can compare the energy densities of the squeezing W_{es} and flexing W_{fl}. $W_{es}=\frac{1}{2}\varepsilon_o \varepsilon (\frac{V}{l})^2$ and $W_{fl}=\frac{e_3 V}{Rl}$, where $l \sim 25$ μm is the thickness of the liquid crystal. With the measured $R \sim 1300$ m, $e_3 \sim 50$ nC/m, and $\varepsilon \sim 5 \times 10^{-11}$ Cm^2/V, for example, at 25 V $W_{es}=25$ J/m^3 and $W_{fl}=12$ J/m^3. The difference between W_{es} and W_{fl} is further increasing at higher voltages. In spite of this, in the nematic phase the measured displacements due to electrostatic forces are smaller than that due to bending, because squeezing requires flow of the material from the electrode area, whereas the bending does not require flow. That explains why the squeezing displacement drops in the more viscous nematic with defects, and basically disappears in the rigid crystal phase.

To summarize, we have presented measurements of the converse flexoelectric effect—a polar, field-induced mechanical flexure of a nematic film—in thermotropic liquid crystals using a bent-core mesogen. The value of the flexoelectric coefficient e_3 deduced from these measurements is in satisfactory agreement with direct measurements of the flexoelectric effect based on polarization current measurements under applied curvature strain. In addition these measurements showed that the sign of the bend flexoelectric coefficient is positive. The converse effect could prove quite useful for low-cost, highly processible electromechanical actuators and beam steering devices.

ACKNOWLEDGMENTS

The work was partially supported by Grant Nos. NSF-DMR-0606160, NSF REU B-8513, and ONR-N00014-07-1-0440. We acknowledge useful discussions with N. Éber and A. G. Petrov. We thank J. Kim and Q. Li for supplying the ClPbis10Bb.

[1] T. Niori, T. Sekine, J. Watanabe, T. Furukawa, and H. Takezoe, J. Mater. Chem. **6**, 1231 (1996); T. Sekine, T. Niori, M. Sone, J. Watanabe, S. W. Choi, Y. Takanishi, and H. Takezoe, Jpn. J. Appl. Phys., Part 1 **36**, 6455 (1997); D. R. Link, G. Natale, R. Shao, J. E. Maclennan, N. A. Clark, E. Körblova, and D. M. Walba, Science **278**, 1924 (1997).

[2] J. Matraszek, J. Mieczkowski, J. Szydlowska, and E. Gorecka, Liq. Cryst. **27**, 429 (2000); I. Wirth, S. Diele, A. Eremin, G. Pelzl, S. Grande, L. Kovalenko, N. Pancenko, and W. Weissflog, J. Mater. Chem. **11**, 1642 (2001); W. Weissflog, H. Nádasi, U. Dunemann, G. Pelzl, S. Diele, A. Eremin, and H. Kresse, *ibid.* **11**, 2748 (2001).

[3] E. Mátyus and K. Keserü, J. Mol. Struct. **543**, 89 (2001).

[4] T. J. Dingemans and E. T. Samulski, Liq. Cryst. **27**, 131 (2000).

[5] A. Roy, N. V. Madhusudana, P. Toledano, and A. M. Figureiredo Neto, Phys. Rev. Lett. **82**, 1466 (1999).

[6] H. R. Brand, P. E. Cladis, and H. Pleiner, Eur. Phys. J. B **6**, 347 (1998).

[7] T. C. Lubensky and L. Radzihovsky, Phys. Rev. E **66**, 031704 (2002); L. Radzihovsky and T. C. Lubensky, Europhys. Lett. **54**, 206 (2001).

[8] H. R. Brand, H. Pleiner, and P. E. Cladis, Eur. Phys. J. E **7**, 163 (2002).

[9] D. B. Wiant, J. T. Gleeson, N. Éber, K. Fodor-Csorba, A. Jákli, and T. Tóth-Katona, Phys. Rev. E **72**, 041712 (2005).

[10] D. Wiant, S. Stojadinovic, K. Neupane, S. Sharma, K. Fodor-Csorba, A. Jákli, J. T. Gleeson, and S. Sprunt, Phys. Rev. E **73**, 030703(R) (2006).

[11] E. Dorjgotov, K. Fodor-Csorba, J. T. Gleeson, S. N. Sprunt, and A. Jákli, Liq. Cryst. **35**, 149 (2008).

[12] J. Harden, B. Mbanga, N. Éber, K. Fodor-Csorba, S. Sprunt, J. T. Gleeson, and A. Jákli, Phys. Rev. Lett. **97**, 157802 (2006).

[13] R. B. Meyer, Phys. Rev. Lett. **22**, 918 (1969).

[14] J. Y. Fu, W. Zhu, and L. E. Cross, J. Appl. Phys. **100**, 024112 (2006).

[15] A. T. Todorov, A. G. Petrov, and J. H. Fendler, J. Phys. Chem. **98**, 3076 (1994).

[16] A. G. Petrov, M. Spassova, and J. H. Fendler, Thin Solid Films **285**, 845 (1996).

[17] A. G. Petrov, Anal. Chim. Acta **568**, 70 (2006).

[18] A. Derzhanski, A. G. Petrov, A. T. Todorov, and K. Hristova, Liq. Cryst. **7**, 439 (1990).

[19] K. Fodor-Csorba, A. Vajda, G. Galli, A. Jákli, D. Demus, S. Holly, and E. Gács-Baitz, Macromol. Chem. Phys. **203**, 1556 (2002); K. Fodor-Csorba, A. Jákli, and G. Galli, Macromol. Symp. **218**, 81 (2004).

[20] G. Pelzl, A. Eremin, S. Diele, H. Kresse, and W. Weissflog, J. Mater. Chem. **12**, 2591 (2002); W. Weissflog *et al.*, Liq. Cryst. **31**, 923 (2004).

[21] O. Kafri, Opt. Lett. **14**, 657 (1989).

[22] A. Ansari and J. F. Marko, Lecture Notes Molecular and Cellular Biophysics, http://www.uic.edu/classes/phys/phys461/phys450/MARKO/N016.html

[23] T. J. Ma *et al.*, Rev. Sci. Instrum. **73**, 1813 (2002).

[24] K. Matsuzawa, J. Acoust. Soc. Jpn. **15**, 147 (1959).

[25] K. Matsuzawa, J. Acoust. Soc. Jpn. **15**, 147 (1959).

[26] A. Jákli, M. Chambers, J. Harden, M. Majumbar, R. Teeling, J. Kim, Q. Li, G. G. Nair, N. Éber, K. Fodor-Csorba, J. T. Gleeson, and S. Sprunt, Proc. SPIE **6911**, 5 (2008).